Flat bands and dynamical localization of spin-orbit-coupled Bose-Einstein condensates

Fatkhulla Kh. Abdullaev
Physical-Technical Institute, Uzbekistan Academy of Sciences, Tashkent, Uzbekistan

Mario Salerno
Dipartimento di Fisica "E.R. Caianiello" and Istituto Nazionale di Fisica Nucleare - Gruppo Collegato di Salerno, Universitá di Salerno, Via Giovanni Paolo II, 84084 Fisciano (SA), Italy

(Received 8 August 2018; published 5 November 2018)

Flat bands and dynamical localization of binary mixtures of Bose-Einstein condensates, with spin-orbit coupling subjected to a deep optical lattice which is shaking in time and to a periodic time modulation of the Zeeman field, are investigated. In contrast with usual dynamical localization in the absence of spin-orbit coupling, we find that to fully suppress the tunneling in the system the optical lattice shaking is not enough, and a proper tuning of the spin-orbit term, achievable via the Zeeman field modulation, is also required. This leads to a sequence of Zeeman parameter values where energy bands become flat, the tunneling in the system is suppressed, and the dynamical localization phenomenon occurs. Exact wave functions at the dynamical localization points show that the binary mixture localizes on a dimer with the two components occupying different sites. This type of localization occurs in exact form also for the ground state of the system at the dynamical localization points in the presence of nonlinearity and remains valid, although in approximate form, for a wide range of the Zeeman parameter around these points. The possibility of observing the above phenomena in real experiments is also briefly discussed.

DOI: 10.1103/PhysRevA.98.053606

I. INTRODUCTION

Significant attention is presently devoted to the study of time-periodically driven many-body systems [1,2] that exhibit interesting transport phenomena that resemble the ones observed in condensed matter physics under the action of static or time-periodic electric fields. In this context, it is well known that a constant electric field cannot induce transport in perfect crystals, due to the phenomenon of Bloch oscillations. In the presence of a time-periodic electric field, however, transport becomes generically possible, except for specific ratios of the field amplitude and frequency for which the phenomenon of dynamical localization (DL) appears.

As first demonstrated in Ref. [3] for the Schrödinger tight-binding model of electrons in perfect crystals, DL emerges due to the tunneling suppression between adjacent sites induced by the periodic electric field. For harmonic fields this happens when the amplitude frequency ratio matches zeros of the Bessel function J_0. DL is not a peculiarity of linear systems but exists also in the presence of nonlinearity (interactions), as has been shown for the discrete nonlinear Schrödinger equation (DNLS) in Ref. [4] and its quantum version (Bose-Hubbard model) in Ref. [5]. To date, DL has been observed in many physical systems, among which are spin chains [1], periodically curved arrays of optical waveguides [6,7], and cold atoms loaded in shaken optical lattices [8].

In Bose-Einstein (BEC) condensates, the analogs of periodic electric fields can be realized by means of shaking optical lattices. This leads to very interesting phenomena including the generation of synthetic gauge fields [9], topological insulators [10], etc. In these systems it is also possible to modulate the interactions (scattering lengths) in time, a fact that allows one to change the inter-site tunneling of BEC in optical lattices in a manner that depends not only on the amplitude and frequency of the modulation but also on the relative atomic imbalance between adjacent sites [11,12]. This leads to the appearance of new quantum phases [13], density dependent gauge fields [14], and matter wave excitations localized on a compact domain (compactons) [12,15]. Time-dependent modulations of the scattering lengths have been also shown to be very effective to suppress dynamical instabilities and to induce long-living Bloch oscillations [16] and DL [17] of matter-wave gap solitons.

Spin-orbit coupling (SOC) opens new possibilities for investigating the above phenomena in BEC systems. In particular, due to the interplay between SOC, periodicity, and nonlinearity, DL could display interesting new features. In BEC systems the effective SOC stemming from internal atomic states which are coupled by Raman laser fields [18] can be tuned by means of fast and coherent modulations of the laser intensities [19]. This can be achieved via modulations of the Raman term, as experimentally demonstrated in Ref. [20], by modulating gradient magnetic fields [21], or by time-periodic modulations of the Zeeman field [22].

In spite of this, however, very few investigations of flat bands and DL for SOC-BEC systems presently exist. In this context we mention the spin-dependent DL of a SOC single atom in a driven optical bipartite lattice [23], the DL in a SOC two-level atom trapped in periodic potential under the action of weak harmonically varying linear force [24], and the dynamical suppression of the tunneling in a double well potential for a noninteracting (linear) SOC-BEC system [25]. Moreover, almost no studies exist on the effect of combined modulations on the DL phenomenon. In this respect we can

mention only the work [26], where combined modulations of interactions and lattice shaking are used to generate the extended Hubbard models with asymmetric hopping which predict new quantum phases in BEC.

The aim of the present paper is to investigate DL phenomena in binary BEC mixtures subjected to optical lattice shaking, time-periodic Zeeman field, and equal SOC contributions of Rashba and Dresselhaus type. For this we use a tight binding model for BEC-SOC mixture appropriate for deep optical lattices [27,28] and treat the time modulations in the fast frequency limit. This leads to an effective time-averaged Hamiltonian system which can be analytically solved in the linear case and analytically (at DL points) and numerically investigated in the nonlinear case.

As a result we find that, in contrast with usual DL (e.g., in absence of SOC), the shaking of the optical lattice alone is not enough to fully suppress the tunneling, and suitable tunings of the SOC term with the optical lattice shaking, achieved via Zeeman field modulation, are also required. This leads to a sequence of Zeeman parameter values for which DL can occur (DL points). We show that at DL points the energy bands become flat and the tunneling is fully suppressed. In the linear case, exact wave functions derived at the DL points show that the localization occurs on a dimer with the BEC components occupying different sites. We show that this holds true, in exact form, also for the ground state wave functions at the DL points in the presence of contact interactions, and it remains valid, in approximate form, for a wide range around these points.

The paper is organized as follows. In Sec. II we introduce the model equations and derive the effective averaged Hamiltonian system. In Sec. III we study the dispersion relation and the linear spectrum as a function of the system parameters. In Sec. IV exact analytical wave functions at the DL points of the linear case are derived and in Sec. V we extend results to the ground state of the system in the presence of nonlinearity. Finally, in Sec. VI we discuss parameters design for possible experiments and briefly summarize the main results of the paper.

II. MODEL AND AVERAGED EQUATIONS

A BEC with equal Rashba and Dresselhaus SOC contributions loaded in a deep optical lattice can be described in the mean field approximation by the following DNLS equation [27,28]:

$$\begin{aligned} i\frac{du_n}{dt} &= -\Gamma(u_{n+1}+u_{n-1}) + i\frac{\sigma}{2}(v_{n+1}-v_{n-1}) \\ &\quad + \Omega u_n + (\gamma_1|u_n|^2+\gamma|v_n|^2)u_n + f(t)nu_n, \\ i\frac{dv_n}{dt} &= -\Gamma(v_{n+1}+v_{n-1}) + i\frac{\sigma}{2}(u_{n+1}-u_{n-1}) \\ &\quad - \Omega v_n + (\gamma|u_n|^2+\gamma_2|v_n|^2)v_n + f(t)nv_n. \end{aligned} \quad (1)$$

Here σ and Ω denote the SOC and the Zeeman parameters while the linear ramp potential, modeling the optical lattice shaking, is assumed to be time-periodic with amplitude $f(t) = f_0\cos(\omega t)$. In order to have SOC tunability we also assume that the Zeeman term is varying periodically in time as $\Omega = \Omega(t) = \Omega_0 + \Omega_1\cos(\omega t)$, where Ω_0 is a constant fixed part and Ω_1 is the amplitude of the part that is modulated with the same frequency ω of the lattice shaking. In the following we assume rapid and strongly varying fields, $\Omega(t)$, $f(t)$, of the form

$$\Omega(t) = \Omega_0 + \frac{1}{\epsilon}\Omega_1\cos(\omega\tau), \qquad f(t) = \frac{1}{\epsilon}f_0\cos(\omega\tau), \quad (2)$$

with $\epsilon \ll 1$ and $\tau = \frac{t}{\epsilon}$ denoting a fast time variable. To remove the explicit fast time dependence from Eq. (1) it is convenient to perform the following transformation:

$$u_n = U_n e^{-i\frac{\sin(\omega t)}{\omega}(\Omega_1+\gamma_0 n)}, \qquad v_n = V_n e^{i\frac{\sin(\omega t)}{\omega}(\Omega_1-\gamma_0 n)}. \quad (3)$$

By substituting into Eq. (1) and averaging with respect to the fast time variable we obtain the following averaged system:

$$\begin{aligned} i\dot{U}_n &= -\Gamma J_0(\chi)(U_{n+1}+U_{n-1}) + \frac{i\sigma}{2}(J_0^- V_{n+1} - J_0^+ V_{n-1}) \\ &\quad + \Omega_0 U_n + (\gamma_1|U_n|^2+\gamma|V_n|^2)U_n, \\ i\dot{V}_n &= -\Gamma J_0(\chi)(V_{n+1}+V_{n-1}) + \frac{i\sigma}{2}(J_0^+ U_{n+1} - J_0^- U_{n-1}) \\ &\quad - \Omega_0 V_n + (\gamma_2|V_n|^2+\gamma|U_n|^2)V_n, \end{aligned} \quad (4)$$

where $J_0(\chi)$ denotes the zero-order Bessel function of a variable χ, while $J_0^{\pm}$ stands for

$$J_0^{\pm} \equiv J_0^{\pm}(\eta) = J_0(\eta \pm \chi) \quad (5)$$

with

$$\chi = \frac{f_0}{\omega}, \qquad \eta = 2\frac{\Omega_1}{\omega}.$$

Notice that Eq. (4) has two conserved quantities: the norm

$$N = \sum_n (|U_n|^2 + |V_n|^2) \quad (6)$$

and the Hamiltonian (energy)

$$\begin{aligned} H = \sum_n \Big\{ &-J_0(\chi)\Gamma(U_n^* U_{n+1} + V_n^* V_{n+1}) \\ &+ i\frac{\sigma}{2}U_n^*(J_0^- V_{n+1} - J_0^+ V_{n-1}) \\ &+ \frac{\Omega_0}{2}(|U_n|^2 - |V_n|^2) + \text{c.c.}\Big\} + E_{\text{int}}, \end{aligned}$$

where E_{int} is the interaction energy,

$$E_{\text{int}} = \sum_n \left\{ \frac{1}{2}(\gamma_1|U_n|^4 + \gamma_2|V_n|^4) + \gamma|U_n|^2|V_n|^2 \right\}, \quad (7)$$

and c.c. denotes the complex conjugate of the expression in the curly brackets. From Eq. (4) it is clear that the interwell tunneling induced by the dispersive term Γ can be suppressed if χ is taken as a zero of the Bessel function J_0. Notice that in absence of SOC this would be sufficient to fully suppress the tunneling in the system but in the presence of SOC this is not so because tunneling remains possible through the σ term in Eq. (4).

III. DISPERSION RELATIONS AND LINEAR ENERGY SPECTRUM

In the absence of contact interactions [$\gamma = \gamma_1 = \gamma_2 = 0$ in Eq. (4)] it is possible to derive the dispersion relation by assuming a dependence of U_n, V_n on time and on the lattice site n of the form

$$U_n(t) = A \exp i(kn - \epsilon t), \quad V_n(t) = B \exp i(kn - \epsilon t), \quad (8)$$

where A, B are real constants, k is the crystal momentum varying in the first Brillouin zone, $k \in [-\pi, \pi]$, and ϵ has the physical meaning of chemical potential ($\equiv$ energy in linear case). The dispersion relation, e.g., the dependence of ϵ on k, directly follows from the compatibility condition of the resulting linear system, and one can easily show that it leads to

$$\epsilon_\nu(k) = -2\Gamma J_0(\chi)\cos(k) + \nu\sqrt{\Omega_0^2 + \frac{\sigma^2}{4}[J_0^+(\eta) - J_0^-(\eta)]^2 + \sigma^2 J_0^+(\eta) J_0^-(\eta)\sin(k)^2} \quad (9)$$

with the index ν assuming the values $\nu = -1, 1$, in correspondence with the lower and upper branches of the dispersion curve, respectively.

Notice that in the absence of modulations (e.g., $f_0 = \Omega_1 = \eta = \chi = 0$) we have $J_0(\eta) = J_0^\pm = 1$ and the above dispersion relation reduces the the one in Ref. [27] for the case of a static optical lattice and constant Zeeman field. Similarly, in absence of the shaking of the optical lattice (e.g., for $f_0 = \chi = 0$), Eq. (9) reproduces the one considered in Ref. [22] for the case of SOC tunability induced by time dependent Zeeman fields. Typical dispersion curves for different modulating parameter values are depicted in Fig. 1. Notice from the bottom panel the occurrence of a flat band for the value $\eta = 4.809\,65$, which is related to a zero of the Bessel function J_0 as we shall see in the following.

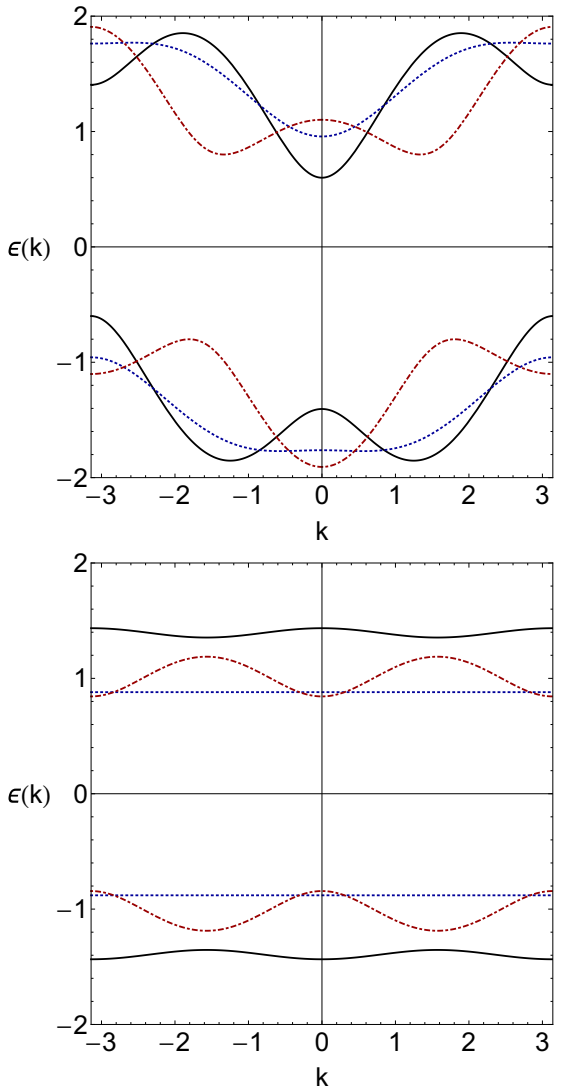

FIG. 1. Typical dispersion curves of the linear SOC-DNLS system ($g = 0$) for two values of the optical lattice shaking parameter, $\chi = 1.2$ (top panel) and $\chi = \xi_1 = 2.40483$ (bottom panel), and different Zeeman field modulations. The black continuous, blue dotted, and red dot-dashed curves in the top and bottom panels refer to $\eta = 0.5, 1.0, 2.5$, and $\eta = 3.0,\ 4.809\,65,\ 5.0$, respectively. Other parameters are fixed as $\Gamma = 0.3,\ \Omega_0 = 0.8,\ \sigma = 2.5$.

IV. SOC DYNAMICAL LOCALIZATION: LINEAR CASE

In this section we consider the effects of the optical lattice shaking and Zeeman modulation on the band flatness, suppression of tunneling, and DL existence, in the absence of any contact interaction. To this end we fix the optical lattice shaking parameter χ to a zero of the Bessel function, say $\chi = \bar{\xi}$, so that the effective inter-well tunneling constant, $J_0(\chi)\Gamma$, vanishes. In this case the lower and upper bands are related by the symmetry $\epsilon_1(k) = -\epsilon_{-1}(k)$, and their dependence on k is fully controlled by the Zeeman parameter η through the factor $\sigma^2 J_0^+ J_0^-$ in Eq.(9).

Considering the SOC parameter different from zero, we have that the band flatness is achieved when one of the equations: $J_0^\pm(\eta) \equiv J_0(\eta \pm \bar{\xi}) = 0$, is satisfied. This occurs for η taken as

$$\eta_n^\pm = \xi_n \pm \bar{\xi}, \quad (10)$$

with ξ_n, $n = 1, 2, \ldots$ denoting the nth zero of J_0. Flat bands in k-space are found in correspondence with the N-fold degenerate eigenvalues

$$\epsilon_\nu = \nu\sqrt{\Omega_0^2 + \frac{\sigma^2}{4} J_0^\pm(\eta_n^\pm)^2}, \quad (11)$$

which depend on σ and with $\nu = -1, 1$ referring to the lower and upper bands, respectively. From this it follows that for $\chi = \bar{\xi} \equiv \xi_m$, the mth zero of J_0, the band flatness occurs in correspondence with the sequence of η values (DL points), listed in increasing order,

$$\{\eta_m^-, \eta_{m+1}^-, \ldots, \eta_{2m}^-, \eta_1^+, \eta_{2m+1}^-, \eta_2^+, \eta_{2m+2}^-, \eta_3^+, \eta_{2m+3}^-, \ldots\}. \quad (12)$$

Thus, for $m = 1$, e.g. $\chi = \xi_1 = 2.404\,83$, the first zero of J_0, the η sequence is

$$\{\eta_1^-, \eta_2^-, \eta_1^+, \eta_3^-, \eta_2^+, \eta_4^-, \eta_3^+, \eta_5^-, \eta_4^+, \eta_6^-, \eta_5^+, \eta_7^-, \dots\}. \tag{13}$$

Notice that the flat band depicted in the bottom panel of Fig. 1 just corresponds to the η_1^+ value in the above sequence. Also notice that at DL points the band velocity $v = d\epsilon(k)/dk$ vanishes for all values k, so the transport is fully suppressed and DL occurs.

In Fig. 2 we report the energy spectrum as a function of the modulation parameter η for χ fixed as the first (top panel) and second (bottom panel) zeros of J_0. In both cases the effective interwell tunneling $J_0(\chi)\Gamma$ vanishes and we see the shrinking of the spectrum into two degenerate points exactly at the values predicted by Eq. (12). Notice that the degenerate energies at these points correspond to different values of the crystal momentum k and generate the upper and lower flat bands seen in the bottom panel of Fig. 1, when plotted in k-space.

In Fig. 3 we show the energy spectrum as in Fig. 2 but for χ slightly different from a zero of J_0. Since the effective interwell tunneling is not zero, no shrinking of the spectrum into single points can be observed in this case. Obviously, no flat bands, tunneling suppression, or DL phenomena can arise for any value of η.

Notice that when the Zeeman field modulation is switched off, e.g. $\eta = 0$, the flatness of the bands and the DL phenomenon occur when the intrawell tunneling is suppressed, e.g., when χ matches a zero of J_0. In this case, however, $J_0^{\pm} = J_0(\chi) = 0$ so there are only the trivial flat bands $\epsilon_\nu = \nu\Omega_0$ and no SOC contribution to the DL at all, since σ disappears from the dispersion relation. From this it is clear that in the presence of SOC the suppression of the interwell tunneling by means of the optical lattice shaking alone is not enough to induce DL, and the matching of the Zeeman field parameters with the values in Eq. (12) is absolutely necessary for DL and band flatness to exist.

Let us now investigate the eigenstates of the system at the DL points. In this respect, we remark from Eq. (4) that for $J_0(\chi) = 0$ and η satisfying one of the two equations $J_0^{\pm}(\eta) = 0$, the system reduces to a chain of uncoupled dimers described by the equations

$$i\dot{A} \mp \frac{i\sigma}{2} J_0^{\mp} B - \Omega_0 A = 0, \quad i\dot{B} \pm \frac{i\sigma}{2} J_0^{\mp} A + \Omega_0 B = 0, \tag{14}$$

with A, B standing for $U_n, V_{n\pm1}$ and the signs appearing in the equations related to which of the two equations $J_0^{\pm} = 0$ is satisfied by η. In this case one can readily check that the following stationary dimer solution exists:

$$A_\nu \equiv U_n = -2i\sqrt{\frac{(\epsilon_\nu + \Omega_0)(\epsilon_\nu^2 - \Omega_0^2)}{2\epsilon_\nu(\sigma J_0^{\mp})^2}}\, e^{-i\epsilon_\nu t}\delta_{n,n_0}, \tag{15}$$

$$B_\nu \equiv V_n = -\nu\sqrt{\frac{\epsilon_\nu - \Omega_0}{2\epsilon_\nu}}\, e^{-i\epsilon_\nu t}\delta_{n,n_0\pm1}, \tag{16}$$

with ϵ_ν being the flat band energy at the DL point in Eq. (11).

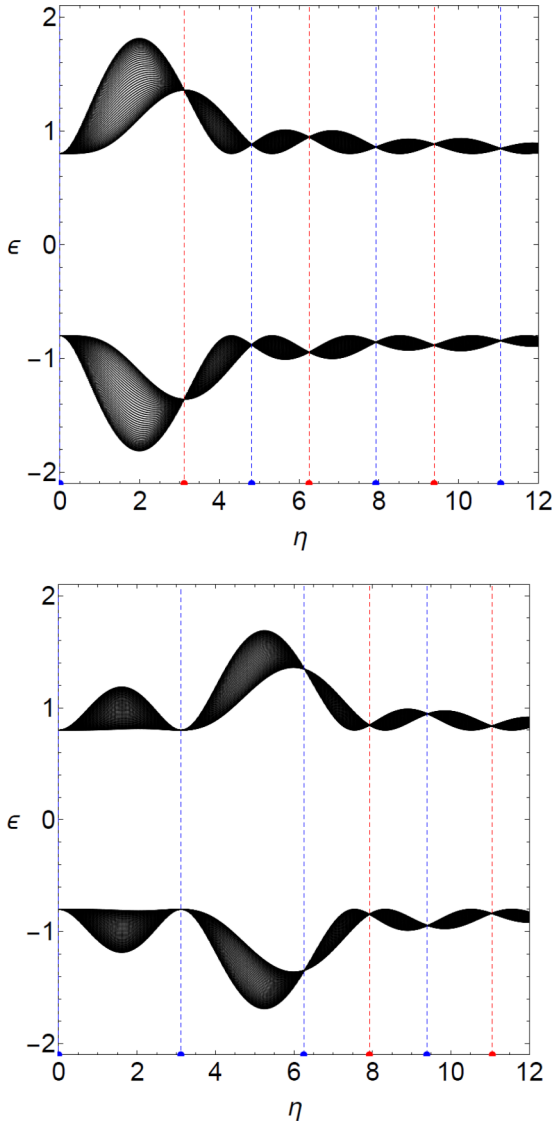

FIG. 2. Energy spectrum versus η for parameter χ fixed as the first (top panel) and second (bottom panel) zeros of the Bessel function J_0, e.g., $\chi = 2.404\,83$ and $\chi = 5.520\,08$, respectively. Blue and red dots correspond to the η^- and η^+ values (e.g., to solutions of the equations $J^+ = 0$ and $J^- = 0$, respectively), leading to the sequences in Eq. (12): {0, 3.115 25, 4.809 65, 6.2489, 7.9249, 9.386 71, 11.0586} (top panel) and {0, 3.133 65, 6.271 46, 7.9249, 9.410 84, 11.0402} (bottom panel). Dashed blue and red lines have been drawn just as a guide for the eyes through the band shrinking points. The full spectrum for a given η has been derived for a chain of 99 sites. Other parameters are fixed as in Fig. 1.

Notice that the above eigenstates are normalized according to $|A|^2 + |B|^2 = 1$ and they can exist, on any lattice point, for a total of N orthonormal states per band (N being the number of lattice sites in the chain). Actually, from this complete set of localized states one can construct extended (Bloch) states at the DL points in terms of a Fourier transform. The fact that the two components of the above dimer solution are localized on different sites implies that they exist also in the presence of the intraspecies interactions, e.g., at the DL points the

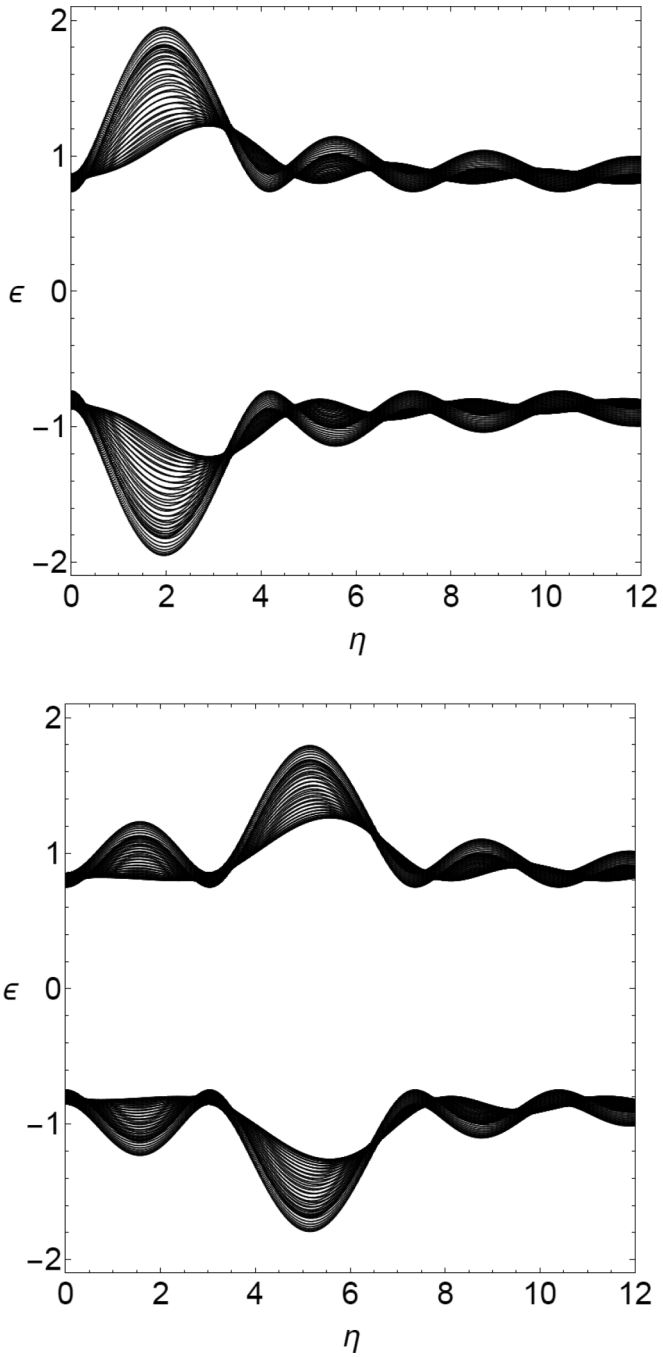

FIG. 3. Energy spectrum versus η as in Fig. 2 but for χ detuned from the first two zeros of J_0 by -0.25, e.g., $\chi = \xi_i - 0.25$ with $i = 1, 2$ for top and bottom panels respectively. Other parameters are fixed as in Fig. 2.

SOC system remains dimerized even in the presence of the interspecies nonlinearity if the nonlinearity intrasite scattering lengths are detuned to zero.

V. SOC DYNAMICAL LOCALIZATION: NONLINEAR CASE

In the presence of contact interactions the spectrum cannot be computed analytically, but it can be computed numerically, with high accuracy, by means of self-consistent diagonalization (SCD) procedure [29]. Quite surprisingly, we find that

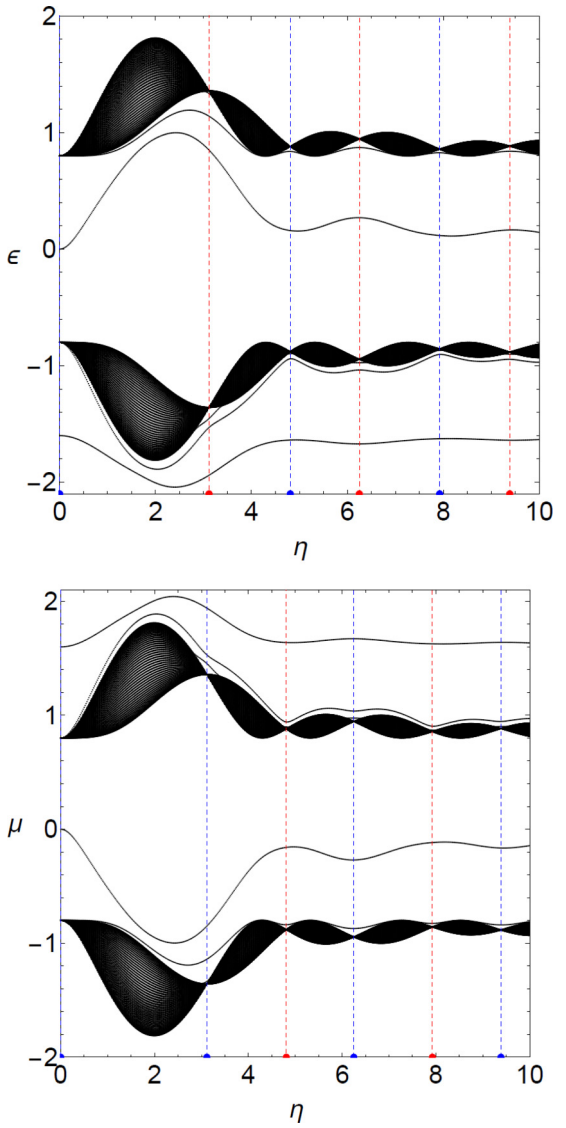

FIG. 4. Chemical potential $\mu = \epsilon + E_{\rm int}$ for the equally attractive case $\gamma_1 = \gamma_2 = \gamma = -0.8$ (top panel) and the equally repulsive case $\gamma_1 = \gamma_2 = \gamma = 0.8$ (bottom panel). Other parameters are fixed as $\chi = \xi_1 = 2.404\,83$, $\Gamma = 0.3$, $\Omega_0 = 0.8$, $\sigma = 2.5$.

the results of the previous section for DL points survive in the presence of nonlinearity. This is shown in Fig. 4 where the spectrum of the Hamiltonian versus η is depicted for the cases of all attractive interactions (top panel) and all repulsive interactions (bottom panel). We see that, except for the presence of additional nondegenerate bound state curves introduced by the interactions, both in the semi-infinite and interband gaps, the top and bottom bands curves are very similar to the ones depicted in Fig. 2, shrinking into single points and leading to flat bands in k-space, at exactly the same values of η derived in Eq. (12) for the linear case (similar results are found for other values of the nonlinearity parameters). The fact that the DL points are unaffected by the interaction is a consequence of the dimer localization and of the onsite nonlinearity.

From Fig. 4 it is also clear that while in the attractive case the degeneracy of the ground state at the DL points is fully removed by the nonlinearity, in the repulsive case the ground

state remains highly degenerate and almost unaffected by the interaction (see bottom panel of Fig. 4). We remark that, in analogy with gap solitons of the continuous Gross-Pitaevskii equation [30], the nondegenerate localized states which appear in the band gaps originate from linear Bloch states at the center (resp. edges) of the Brillouin zone that become modulationally unstable when an attractive (resp. repulsive) interaction is switched on. The energies (chemical potentials) of these states, due to their negative (resp. positive) interaction energy contributions, are pulled just below (resp. above) the linear flat band value in the case of attractive (resp. repulsive) interactions. This explains why the ground state degeneracy at the DL points is fully removed for attractive interactions but not for repulsive interactions. The irrelevance of repulsive nonlinearities for flat band ground states also correlates with similar behaviors observed in the pure quantum regime of flat band interacting bosons in the small density limit [31].

In the following we restrict to the case of all attractive interactions and concentrate on the ground state curve shown in the top panel of Fig. 4. In this respect we remark that the ground states at the DL points can be computed exactly by assuming the same type of dimerized localization found in the linear case. In this respect let us look for states localized on two sites of the form $U_{n_0} = ae^{-i\epsilon t}$, $V_{n_0+1} = ibe^{-i\epsilon t}$ with a, b real constants and with $U_n = 0$, and $V_n = 0$ on all other sites different from n_0 and $n_0 + 1$, respectively. Substituting into Eq. (4) and looking for stationary solutions, we obtain the following cubic system:

$$\tfrac{1}{2}\sigma J_0^+ b - (\mu - \Omega_0)a + \gamma_1 a^3 = 0, \tag{17}$$

$$\tfrac{1}{2}\sigma J_0^+ a - (\mu + \Omega_0)b + \gamma_2 b^3 = 0, \tag{18}$$

which can be solved, together with the normalization condition $a^2 + b^2 = 1$, exactly for a, b, μ, with $\mu = \epsilon + E_{\rm int}$ denoting the chemical potential. Here we assumed η to be a solution of the equation $J_0^- = 0$, but results for the case $J_0^+ = 0$ follow in similar manner. From this we obtain exact nonlinear localized states at the DL points and, although the analytical expressions for a, b are too involved to be reported, it is possible to obtain them numerically with high accuracy. Despite these results being strictly valid at the DL points where bands are flat, the above equations can be solved in general by considering η a varying parameter, to see how results deviate (away from DL points) from the ones obtained by SCD in Fig. 4. This is shown in Fig .5 for the ground state energy curve. Quite remarkably, we see that the comparison with the SCD curve in Fig. 4 is exact at the DL points and very good for a wide interval, at least up to $\eta \approx 4$.

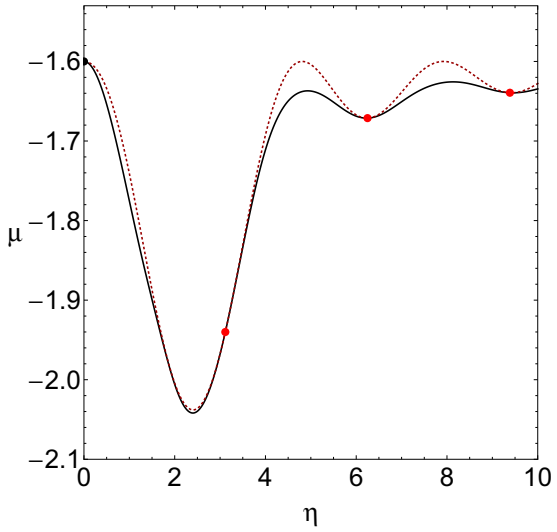

FIG. 5. Comparison between the exact nonlinear ground state curve in Fig. 4 (black solid line) and the corresponding approximated one obtained from Eq. (18) (red dotted line). Notice that the two curves coincide at the DL points (red dots) and are in very good agreement both around these points and in the range $0 < \eta \approx 4$. All parameters are the same as in Fig. 4.

VI. DISCUSSION AND CONCLUSIONS

We briefly discuss possible parameters design and experimental setting to observe the above results presented in this paper. In this respect we refer to the SOC for the case of ^{87}Rb atoms in the field of three laser beams implemented in a tripod scheme. The ground states from the $5S_{1/2}$ manifold are coupled via differently polarized light, by choosing $|1\rangle = |F = 2,\ m_F = -1\rangle$, $|2\rangle = |F = 2,\ m_F = +1\rangle$, and $|3\rangle = |F = 1,\ m_F = 0\rangle$ [32].

The optical lattice can be generated with two additional counterpropagating linearly polarized laser beams of wavelength $\lambda = 2\pi/k_L = 842$ nm with a strength of the order of $10E_R$, with E_R the recoil energy $E_R = \hbar^2 k^2/(2m)$. These values guarantee the applicability of the tight-binding model we used. The passage of the optical lattice laser beams through an acousto-optic modulator permits one to introduce a frequency difference between them which can be used for the shaking of the lattice as discussed in Ref. [33]. The strong modulation limit can be reached by considering a Zeeman field of normalized amplitude >20 and frequency of the modulation fixed by $\omega = 2\Omega_1/\eta$. Under these circumstances, it should be possible to observe the described results and in particular the dimer localization properties of the ground state at the DL points.

In conclusion, we have discussed flat bands, tunneling suppression, and DL in binary BEC mixtures with spin-orbit coupling subjected to a shaking optical lattice and periodic time modulations of the Zeeman field. For this we have used a tight binding model of the BEC mixture valid for deep optical lattices and considered the effects of the modulations by means of the averaging method. In particular, we showed that the suppression of the interwell tunneling is not enough to observe the DL phenomenon, and a suitable tuning of the SOC parameter with the optical lattice shaking is required. The SOC tuning, achieved via the Zeeman field, was shown to lead to a series of parameter values at which flat bands and DL can occur.

Exact analytical expressions of the BEC wave functions at the DL points have been derived, both in absence (linear case) and and in presence (nonlinear case) of interactions. In the latter case we have shown that the dimer localization occurs also for the ground state of the system, in exact form at DL points and in a very good approximation around these points. Parameter designs for possible experimental implementations of the above phenomena were also briefly discussed.

ACKNOWLEDGMENT

M.S. acknowledges partial support from the Ministero dell'Istruzione, dell'Universitá e della Ricerca (MIUR) through the PRIN (Programmi di Ricerca Scientifica di Rilevante Interesse Nazionale) grant on "Statistical Mechanics and Complexity": PRIN-2015-K7KK8L.

[1] M. Bukov, L. D'Alessio, and A. Polkovnikov, Adv. Phys. **64**, 139 (2015).
[2] A. Eckardt, Rev. Mod. Phys. **89**, 011004 (2017).
[3] D. H. Dunlap and V. M. Kenkre, Phys. Rev. B **34**, 3625 (1986); **37**, 6622 (1988).
[4] D. Cai, A. R. Bishop, N. Grønbech-Jensen, and M. Salerno, Phys. Rev. Lett. **74**, 1186 (1995).
[5] A. Eckardt, C. Weiss, and M. Holthaus, Phys. Rev. Lett. **95**, 260404 (2005);
[6] S. Longhi, M. Marangoni, M. Lobino, R. Ramponi, P. Laporta, E. Cianci, and V. Foglietti, Phys. Rev. Lett. **96**, 243901 (2006).
[7] R. Iyer, J. S. Aitchison, J. Wan, M. M. Dignam, and C. M. de Sterke, Opt. Express **15**, 3212 (2007).
[8] H. Lignier, C. Sias, D. Ciampini, Y. Singh, A. Zenesini, O. Morsch, and E. Arimondo, Phys. Rev. Lett. **99**, 220403 (2007).
[9] J. Struck, M. Weinberg, C. Ölschläger, P. Windpassinger, J. Simonet, K. Sengstock, R. Öppner, P. Hauke, A. Eckardt, M. Lewenstein, and L. Mathey, Nat. Phys. **9** (2013).
[10] P. Hauke, O. Tieleman, A. Celi, C. Ölschläger, J. Simonet, J. Struck, M. Weinberg, P. Windpassinger, K. Sengstock, and M. Lewenstein, and A. Eckardt, Phys. Rev. Lett. **109**, 145301 (2012).
[11] J. Gong, L. Morales-Molina, and P. Hänggi, Phys. Rev. Lett. **103**, 133002 (2009).
[12] F. Kh. Abdullaev, P. G. Kevrekidis, and M. Salerno, Phys. Rev. Lett. **105**, 113901 (2010).
[13] A. Rapp, X. Deng, and L. Santos, Phys. Rev. Lett. **109**, 203005 (2012).
[14] S. Greschner, G. Sun, D. Poletti, and L. Santos, Phys. Rev. Lett. **113**, 215303 (2014).
[15] J. D'Ambroise, M. Salerno, P. G. Kevrekidis, and F. K. Kh. Abdullaev, Phys. Rev. A **92**, 053621 (2015); F. Kh. Abdullaev, M. S. A. Hadi, M. Salerno, and B. Umarov, *ibid.* **90**, 063637 (2014); J. Phys. B **50**, 165301 (2017).
[16] M. Salerno, V. V. Konotop, and Yu. V. Bludov, Phys. Rev. Lett. **101**, 030405 (2008).
[17] Yu. V. Bludov, V. V. Konotop, and M. Salerno, Europhys. Lett. **87**, 20004 (2009); J. Phys. B **42**, 105302 (2009).
[18] V. Galitski and I. B. Spielman, Nature (London) **494**, 49 (2013).
[19] Y. Zhang, G. Chen, and C. Zhang, Sci Rep. **3**, 1937 (2013).
[20] K. Jimenez-Garcia, L. J. LeBlanc, R. A. Williams, M. C. Beeler, C. Qu, M. Gong, C. Zhang, and I. B. Spielman, Phys. Rev. Lett. **114**, 125301 (2015).
[21] X. Luo, L. Wu, J. Chen, Q. Guan, K. Gao, Z. Xu, L. You, and R. Wang, Sci. Rep. **6**, 18983 (2016).
[22] M. Salerno, F. Kh. Abdullaev, A. Gammal, and L. Tomio, Phys. Rev. A **94**, 043602 (2016).
[23] Y. Luo, G. Lu, C. Kong, and W. Hai, Phys. Rev. A **93**, 043409 (2016).
[24] Y. V. Kartashov, V. V. Konotop, D. A. Zezyulin, and L. Torner, Phys. Rev. A **94**, 063606 (2016).
[25] Y. V. Kartashov, V. V. Konotop, and V. A. Vysloukh, Phys. Rev. A **97**, 063609 (2018).
[26] S. Greschner, L. Santos, and D. Poletti, Phys. Rev. Lett. **113**, 183002 (2014).
[27] M. Salerno and F. Kh. Abdullaev, Phys. Lett. A **379**, 2252 (2015).
[28] P. P. Belicev, G. Gligoric, J. Petrovic, A. Maluckov, L. Hadievski, and B. A. Malomed, J. Phys. B **48**, 065301 (2015).
[29] M. Salerno, Laser Phys. **15**, 620 (2005).
[30] V. V. Konotop and M. Salerno, Phys. Rev. A **65**, 021602(R) (2002).
[31] S. D. Huber and E. Altman, Phys. Rev. B **82**, 184502 (2010); L. G. Phillips, G. De Chiara, P. Ohberg, and M. Valiente, *ibid.* **91**, 054103 (2015); M. Valiente and N. T. Zinner, J. Phys. B **50**, 064004 (2017).
[32] M. J. Edmonds, J. Otterbach, R. G. Unanyan, M. Fleischhauer, M. Titov, and P. Ohberg, New J. Phys. **14**, 073056 (2012).
[33] A. Eckardt, M. Holthaus, H. Lignier, A. Zenesini, D. Ciampini, O. Morsch, and E. Arimondo, Phys. Rev. A **79**, 013611 (2009).